ACCELERATE SINGLE-SHOT DATA ACQUISITIONS USING COMPRESSED SENSING AND FRONSAC IMAGING

Haifeng Wang, R. Todd Constable and Gigi Galiana

Department of Diagnostic Radiology, Yale University, New Haven, CT, USA

ABSTRACT

Nonlinear spatial encoding magnetic (SEM) fields have been studied to complement multichannel RF encoding and accelerate MRI scans. Published schemes include PatLoc, O-Space, Null Space, 4D-RIO, and others, but the large variety of possible approaches to exploiting nonlinear SEMs remains mostly unexplored. Before, we have presented a new approach, Fast ROtary Nonlinear Spatial ACquisition (FRONSAC) imaging, where the nonlinear fields provide a small rotating perturbation to standard linear trajectories. While FRONSAC encoding greatly improves image quality, at the highest accelerations or weakest FRONSAC fields, some undersampling artifacts remain. However, the under-sampling artifacts that occur with FRONSAC encoding are relatively incoherent and well suited to the compressed sensing (CS) reconstruction. CS provides a sparsity-promoting convex strategy to reconstruct images from highly undersampled datasets. The work presented here combines the benefits of FRONSAC and CS. Simulations illustrate that this combination can further improve image reconstruction with FRONSAC gradients of low amplitudes and frequencies.

Index Terms— nonlinear, parallel imaging, compressed sensing, fronsac imaging, single-shot trajectory, magnetic resonance imaging

1. INTRODUCTION

A number of studies have investigated parallel imaging methods that employ nonlinear SEM fields, including PatLoc imaging [1], O-Space imaging [2-6], Null Space Imaging [7], 4D-RIO [8], etc. The O-space and Null Space approaches in particular illustrate the potential to overcome the limitations of conventional linear spatial encoding and enhance encoding efficiency in the presence of multiple receiver coils. Ultimately, this could allow for greater undersampling thereby shortening scan times [9-10].

Recent research has shown that single shot trajectories using dynamic fields [11-16] may more adequately exploit the potential of nonlinear SEM fields. The work we present here is similar to Ref. [13] and [14], in that it uses time varying nonlinear gradients and is specifically designed to generate compressible waveforms. However, unlike Ref. [13] and [14], where most of the encoding is performed with nonlinear gradients, the nonlinear gradients in this scheme provide only a small perturbation to standard encoding. Adding a rotating nonlinear gradient of modest amplitude provides a flexible strategy to enhance standard undersampled gradient trajectories (i.e. linear trajectories such as EPI, Spiral or Rosette).

We have previously presented this strategy, called FRONSAC imaging [15], which includes linear gradients applied on the three standard linear encoding fields, and rotary or sinusoidal gradient moments, applied on two second-order encoding fields. The low amplitudes of the oscillating gradient waveforms minimally contribute to dB/dt and peripheral nerve stimulation. Images were reconstructed using the Kaczmarz algorithm [2-6]. The simulations results illustrate that FRONSAC imaging can improve image quality in accelerated data acquisitions for arbitrary single-shot trajectories by reducing artifacts due to undersampling. Multi-shot linear trajectories can also incorporate the FRONSAC imaging method.

Compressed sensing (CS) allows sparse signals to be sampled below their conventional Nyquist rate. CS uses a nonlinear procedure to recover the undersampled signal exactly if certain criteria are met [17-25]. Generally, CS theory requires the independent sparse signals to satisfy the restricted isometry property (RIP) condition [17-18]. More specifically, the CS approach generally should satisfy that [19], (i) the image is sparse in a transform domain; (ii) the measurement basis is incoherent with the sparse domain (reached through a sparsifying transform); (iii) a nonlinear reconstruction in the sparse domain enforces sparsity.

The CS approach has been combined with parallel imaging methods with conventional k-space acquisitions [26-30]. But some conventional k-space acquisition schemes, such as Radial and Spiral, can produce more incoherence than standard Cartesian sampling [31-34]. Trajectories can be further improved by adding random perturbations to the conventional sampling trajectories [31-34], but this is often limited by available slew rates. CS recon has successfully been applied to O-Space imaging trajectories to reduce the mean squared error of images at high acceleration, as seen in Ref. [35-36]. However, CS has not been applied to improve the incoherence available in FRONSAC imaging, which has previously only been reconstructed using the standard Kaczmarz algorithm [15].

In this paper, we present a hybrid scheme named CS-FRONSAC, which combines FRONSAC imaging and CS recon. FRONSAC can improve incoherence between the measurement basis and the sparsifying basis, making CS recon more favorable. The results shown below illustrate that the proposed combination can improve image quality compared with either method alone [2-6]. Therefore, CS-FRONSAC can further reduce the mean squared error of images at high acceleration.

2. THEORY

2.1. Nonlinear Spatial Encoding

MRI scanners encode the spatial information of objects using linear gradient magnetic field. But spatial encoding can also be performed with nonlinear magnetic field gradients. Nonlinear gradients may provide faster gradient field switching within safety limits, spatially-varying resolution, and improved parallel imaging using field shapes that are complementary to radio frequency (RF) receiver coil profiles, such as PatLoc [1] and O-Space imaging [2-6].

2.2. FRONSAC Imaging

FRONSAC imaging [15] is a flexible scheme to combine linear and second-order SEM fields to improve the image quality of single-shot linear encoding strategies, such as those from heavily undersampled EPI, Spiral, or Rosette trajectories. In this method, standard linear trajectories are applied on the two linear gradient channels, and a rotating gradient is generated by playing sinusoidal gradient waveforms on two second-order encoding fields, 2xy and x^2-y^2. The images are reconstructed using a Kaczmarz algorithm.

If we neglect relaxation effects, the magnetic resonance signal $\mathbf{s}_q$ from the q-th RF channel should satisfy the following equation,

$$s_q = \int_\Omega m(\mathbf{x}) C_q(\mathbf{x}) e^{i\Phi(\mathbf{x},t)} d\mathbf{x} \qquad (1)$$

where, $m(\mathbf{x})$ is the magnetization at location $\mathbf{x} = (x, y)$; $C_q(\mathbf{x})$ is the sensitivity profiles of q-th coil, and the integral is over Ω, which is the region of interest; $\Phi(\mathbf{x}, t)$ is the spatially dependent encoding phase. In FRONSAC imaging, the phase factor $\Phi(\mathbf{x}, t)$ in Eq. (1) becomes,

$$\begin{aligned}\Phi(\mathbf{x},t) = {} & k_x(t)x + k_y(t)y + A\cdot\sin(\omega t)\cdot 2xy \\ & + A\cdot\cos(\omega t)\cdot\left(x^2+y^2\right)\end{aligned} \qquad (2)$$

where A is the maximum amplitude of the second-order gradient waveforms; $k_x(t)$ and $k_y(t)$ are a vector of gradient moments describing the evolution of each linear gradient field over time. The timing diagram of FRONSAC pulse sequence [15] is shown in Fig.1.

Simulations show that FRONSAC imaging can greatly improve many highly undersampled conventional (i.e., linear) imaging schemes, and distinctly eliminate aliasing artifacts allowing for faster imaging speeds. As described in Ref [15], nonlinear gradients spread the sampling in k-space, which allows the sampling of k-space regions that would otherwise be neglected in the undersampled trajectory. The rotation in the FRONSAC gradient then rotates this diffuse sampling function, allowing us to resolve independent values within the sampling functions.

FRONSAC is practical because it provides significant image improvement even at modest nonlinear gradient amplitudes. But even at modest amplitudes, the shortest single shot acquisitions would require high performance gradients to allow rapid switching of the second order gradient fields (2xy, x^2-y^2). Therefore, techniques that reduce under-sampling artifacts with lower amplitude or frequency FRONSAC gradients are desirable.

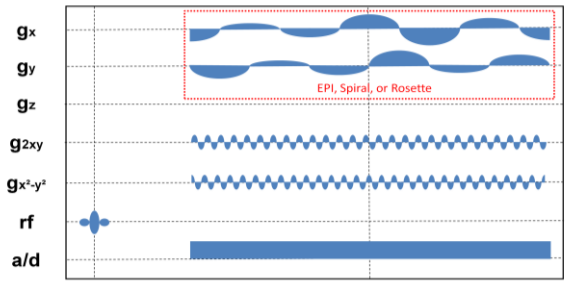

Fig.1 Timing diagram of FRONSAC imaging pulse sequence.

2.3. CS Reconstruction for FRONSAC

To further decrease the requirements of high performance gradients, we apply CS reconstruction instead of pure Kaczmarz reconstruction. According to previous work on the CS reconstruction for O-Space [35-36], we apply the CS reconstruction with the encoding matrix of FRONSAC imaging instead of the conventional Fourier encoding matrix Φ. With this generalization, the equation may be written as:

$$\mathbf{f} = \arg\min\left\{\left\|\Phi\mathbf{f} - \mathbf{s}\right\|_2 + \lambda\left\|\Psi\mathbf{f}\right\|_1\right\} \qquad (3)$$

In the above equation, $\mathbf{f}$ is the desired image signal; $\mathbf{s}$ is the measured signal; $\|\cdot\|_2$ is L-2 norm; $\|\cdot\|_1$ is L-1 norm; Φ is the encoding matrix, i.e. measurement basis or sensing matrix, with its inverse calculated by the Kaczmarz iterative algebraic reconstruction technique, a pseudo-inverse algorithm that converges on the minimum least squares norm solution [2-6]; Ψ is the sparsity transform, such as wavelet, contourlets, finite differences, and so on; λ is the relaxation parameter that controls the convergence properties of the algorithm and is typically set for strongly under-relaxed reconstructions for gradual convergence. The first term imposes data consistency, and the second term encourages sparsity in that domain.

3. METHOD

Simulations were realized in MATLAB using simulated 8-channel receiver coil sensitivity profiles from a single uniform birdcage [35]. A geometric phantom with resolution 128×128, were recovered for the reference (fully sampled

Fourier encoding), FRONSAC, and proposed FRONSAC with CS. Three types of single-shot trajectories, EPI, Spiral and Rosette, as seen in Fig.2, are considered. EPI has 8-fold acceleration; Spiral has 8 cycles with a constant density; Rosette has a single shot trajectory with two frequencies of 98 and 58 Hz if the acquisition time is 25.6 ms [15]. The additional FRONSAC gradient is applied with sinusoid and co-sinusoid waveforms. The details of the CS reconstruction using Kaczmarz are described in Ref [35].

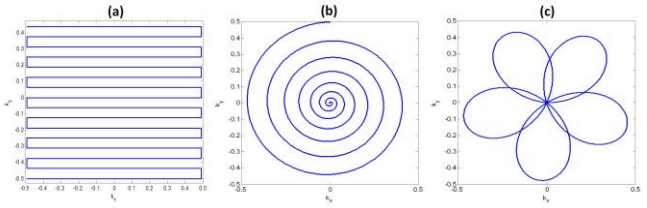

Fig.2 Three types of single-shot trajectories, EPI (a), Spiral (b) and Rosette (c), in k_x-k_y space

4. RESULTS

Fig.3 shows the transform point spread function (TPSF) analysis of EPI and EPI-FRONSAC (⅓ amplitude and ½ frequency of normal values, and both in k_x-k_y space have 4-fold acceleration for 32×32 resolution) in Daubechies wavelet domain. The coarse-scale and fine-scale wavelet coefficients show the peak interferences of the wavelet coefficients are reduced and the aliasing artifacts due to undersampling are incoherent in that transform domain.

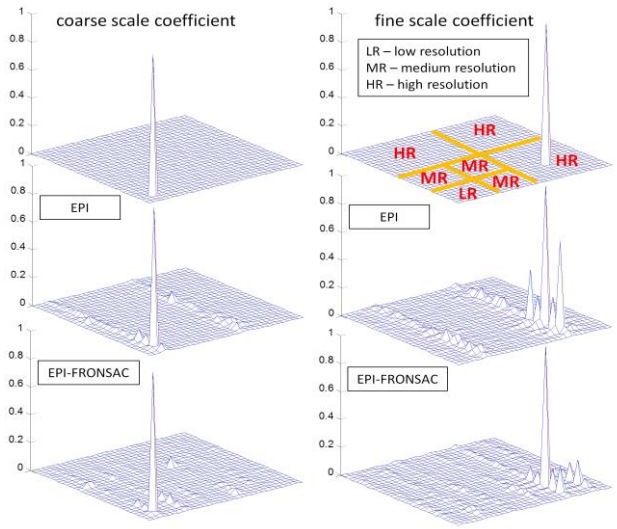

Fig.3 TPSFs of EPI and EPI-FRONSAC in the wavelet domain

Simulations are shown in Fig. 4, comparing 3 trajectories based on EPI (a), Spiral (b) and Rosette (c). The 1st row of panel (a) shows reference and CS recon of a standard EPI acquisition. While CS dramatically reduces artifacts, some ghosted features are clearly visible. Below these images in Fig. 4, results are at modest amplitude and frequency (A and ω, corresponding to A = 790 Hz/cm^2 and $\omega/2\pi$ = 6.4 kHz).

Even without CS reconstruction, the FRONSAC field perturbation greatly improves image quality, however with CS reconstruction; the result closely resembles the reference image. And other panels to the left and below show reconstructions with weaker amplitude and lower frequency FRONSAC gradients, showing that results are greatly enhanced with CS reconstruction.

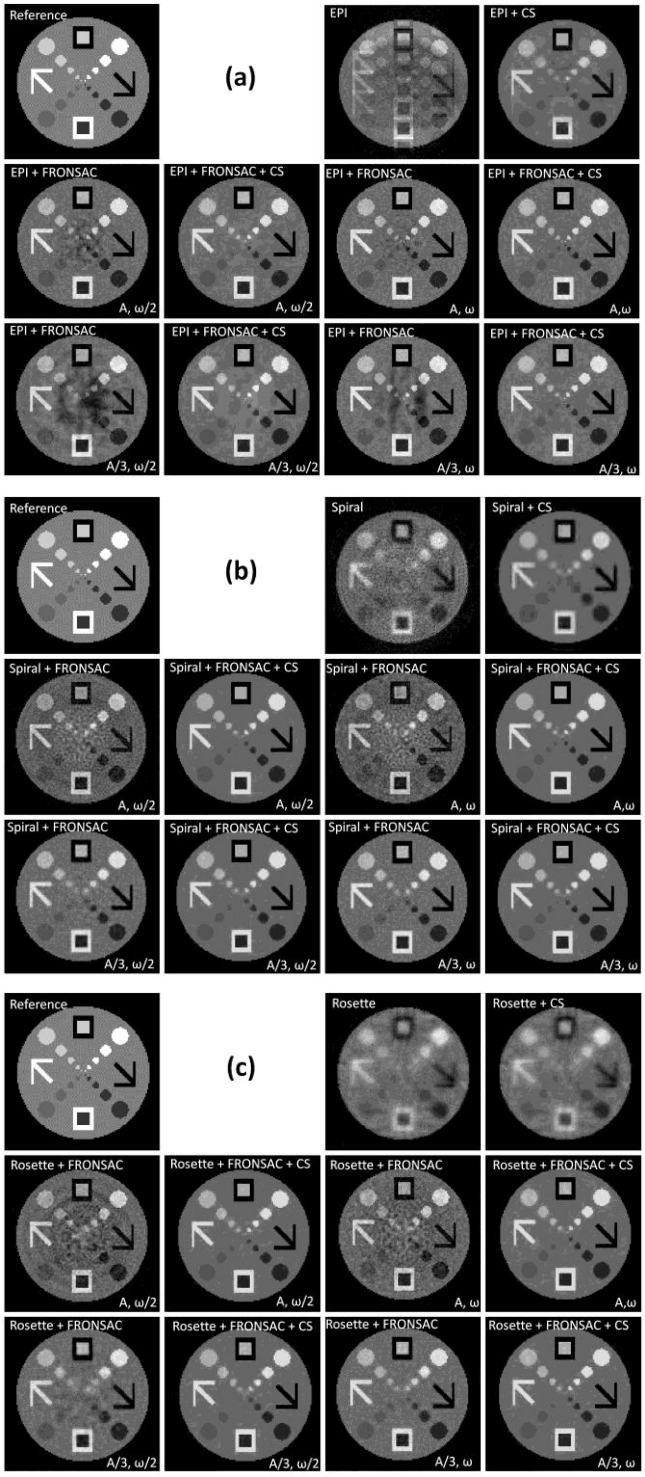

Fig.4 Simulated recon results of EPI (a), Spiral (b) and Rosette (c)

Panels (b) and (c) show analogous reconstructions based on Spiral and Rosette trajectories, respectively. Since the

gaps in k-space are smaller for these linear trajectories, lower values of A and ω are preferable even without CS reconstruction. However, a similar trend is seen where FRONSAC imaging on its own greatly reduces under-sampling artifacts, and the proposed CS-FRONSAC method provides still further improvement, even at lower amplitudes and frequencies.

4. CONCLUSIONS

The CS reconstruction can improve image quality when combined with FRONSAC imaging. The findings illustrate that FRONSAC with small encoding gradients, which minimally contribute to peripheral nerve stimulation (PNS) or gradient hardware demands, can generate excellent image quality from highly undersampled trajectories.

5. REFERENCES

[1] J. Hennig, et al. "Parallel imaging in non-bijective, curvilinear magnetic field gradients: a concept study," *MAGMA*, vol. 21, no. 1-2, pp.5-14, 2008.

[2] J.Stockmann, et al. "O-Space imaging: Highly efficient parallel imaging using second-order nonlinear fields as encoding gradients with no phase encoding," *Magn. Reson. Med.*, vol. 64, no. 2, pp. 447-456, 2010.

[3] J. Stockmann, et al. "In vivo O-Space imaging with a dedicated 12 cm Z2 insert coil on a human 3T scanner using phase map calibration," *Magn. Reson. Med.*, vol. 69, no. 2, pp. 444-455, 2013.

[4] G. Galiana, et al. "Multiecho acquisition of O-space data," *Magn. Reson. Med.*, vol. 72, no. 6, pp. 1648-1657, 2014.

[5] L. Tam, et al. "Prephased O-Space imaging for reduction of asymmetrical local k-space coverage" in Proc. of *ISMRM*, Milan, Italy, pp. 31, 2014.

[6] H. Wang, et al. "Accelerate data acquisition using turbo spin echo and O-space," *Proc. IEEE Int. Symp. Biomed. Imag.*, Beijing, China, pp.874-877, 2014.

[7] L. Tam, et al. "Null space imaging: nonlinear magnetic encoding fields designed complementary to receiver coil sensitivities for improved acceleration in parallel imaging," *Magn. Reson. Med.*, vol. 68, no. 4, pp. 1166-1175, 2012.

[8] D. Gallichan, et al. "Simultaneously driven linear and nonlinear spatial encoding fields in MRI," *Magn. Reson. Med.*, vol. 65, no. 3, pp. 702-714, 2011.

[9] D. Gallichan, et al. "Practical considerations for in vivo MRI with higher dimensional spatial encoding," *MAGMA*, vol. 25, no. 6, pp.419-431, 2012.

[10] G. Galiana, et al. "The role of nonlinear gradients in parallel imaging: A k-space based analysis," *Concepts in Magnetic Resonance Part A*, vol. 40A, no. 5, pp.253-267, 2012.

[11] S. Littin, et al. "Patloc single shot imaging," in Proc. of ISMRM, Salt Lake City, USA, pp.2379, 2013.

[12] F. Testud, et al. "Single-shot imaging with higher-dimensional encoding using magnetic field monitoring and concomitant field correction," *Magn. Reson. Med.*, doi: 10.1002/mrm.25235, 2014.

[13] G. Galiana, et al. "Ultrafast single shot Imaging with rotating nonlinear fields," in Proc. of the *ISMRM*, Salt Lake City, USA, pp. 13, 2013.

[14] G. Galiana, et al. "Single Echo MRI," *PLoS One.*, vol. 9, no.1, pp. e86008, 2014.

[15] H. Wang, et al. "Improving single shot acquisitions with fast rotary nonlinear spatial encoding," in Proc. of *ISMRM*, Milan, Italy, pp.4253, 2014.

[16] K. Layton, et al. "Single shot trajectory design for region-specific imaging using linear and nonlinear magnetic encoding fields," *Magn. Reson. Med.*, vol. 70, no. 3, pp. 684-696, 2013.

[17] E. Candès, et al. "Robust uncertainty principles: Exact signal reconstruction from highly incomplete frequency information," *IEEE Trans. on Info. Theory*, vol. 52, no. 2, pp. 489-509, 2006.

[18] D. Donoho, "Compressed sensing," *IEEE Trans. on Info. Theory*, vol. 52, no. 4, pp. 1289 -1306, 2006.

[19] M. Lustig, et al. "Sparse MRI: The application of compressed sensing for rapid MR imaging," *Magn. Reson. Med.*, vol. 58, no. 2, pp. 1182-1195, 2007.

[20] H. Wang, et al. "Pseudo 2D random sampling for compressed sensing MRI," *Conf. Proc. IEEE Eng. Med. Biol. Soc.*, Minneapolis, USA, pp. 2672-2675, 2009.

[21] D. Liang, et al. "Toeplitz random encoding MR imaging using compressed sensing," *Proc. IEEE Int. Symp. Biomed. Imag.*, Boston, USA, pp. 270-273, 2009.

[22] H. Wang, et al. "Toeplitz random encoding for reduced acquisition using compressed sensing," in Proc. of *ISMRM*, Honolulu, USA, pp.2669, 2009.

[23] J. Haldar, et al. "Compressed-Sensing MRI with random encoding," *IEEE Trans. on Med. Imaging*, vol. 30, no. 4, pp. 893-903, 2011.

[24] G. Puy, et al. "Spread spectrum magnetic resonance imaging," *IEEE Trans. on Med. Imaging*, vol. 31, no. 3, pp. 586-598, 2012.

[25] H. Wang, et al. "Three-dimensional hybrid-encoded MRI using compressed sensing," *Proc. IEEE Int. Symp. Biomed. Imag.*, Barcelona, Spain, pp. 398-401, 2012.

[26] K. Pruessmann, et al. "SENSE: sensitivity encoding for fast MRI," *Magn. Reson. Med.*, vol. 42, no. 5, pp. 952-962, 1999.

[27] M. Griswold, et al. "Generalized autocalibrating partially parallel acquisitions (GRAPPA)," *Magn. Reson. Med.*, vol. 47, no. 6, pp. 1202-1210, 2002.

[28] D. Liang, et al. "Accelerating SENSE using compressed sensing," *Magn. Reson. Med.*, vol. 62, no. 6, pp. 1574-1584, 2009.

[29] M. Lustg, et al. "SPIRiT: Iterative self-consistent parallel imaging reconstruction from arbitrary k-space," *Magn. Reson. Med.*, vol. 64, no. 2, pp. 457-471, 2010.

[30] D. Liang, et al. "Sensitivity encoding reconstruction with nonlocal total variation regularization," *Magn. Reson. Med.*, vol. 65, no. 5, pp. 1384-1392, 2011.

[31] M. Lustig, et al. "Faster imaging with randomly perturbed undersampled spirals and L1 reconstruction," in Proc. of *ISMRM*, Miami, USA, pp.685, 2005.

[32] T. Chang, et al. "MR image reconstruction from sparse radial samples using Bregman iteration," in Proc. of *ISMRM*, Seattle, USA, pp.696, 2006.

[33] A. Bilgin, et al. "Randomly perturbed radial trajectories for compressed sensing MRI," in Proc. of *ISMRM*, Toronto, Canada, pp.3152, 2008.

[34] H. Wang, et al. "Smoothed random-like trajectory for compressed sensing MRI," *Conf. Proc. IEEE Eng. Med. Biol. Soc.*, San Diego, USA, pp. 404-407, 2012.

[35] L. Tam, et al. "Pseudo-random center placement O-space imaging for improved incoherence compressed sensing parallel MRI," *Magn. Reson. Med.*, doi: 10.1002/mrm.25364, 2014.

[36] L. Tam, et al. "Incoherence parameter analysis for optimized compressed sensing with nonlinear encoding gradients," in Proc. of *ISMRM*, Milan, Italy, pp.1559, 2014.